Thermal Properties of Tristearin by Adiabatic and Differential Scanning Calorimetry

Marija Matovic* and J. Cees van Miltenburg

Faculty of Chemistry, Chemical Thermodynamics Group, Debye Institute, Utrecht University, Padualaan 8, 3584 CH Utrecht, The Netherlands

Jan Los

IMM Laboratory of Solid State Chemistry, Radboud University Nijmegen, Toernooiveld, 6525 ED Nijmegen, The Netherlands

Francois G. Gandolfo and Eckhard Flöter

Unilever Research & Development, P.O. Box 114, 3130 AC Vlaardingen, The Netherlands

The thermal behavior of tristearin was studied by adiabatic calorimetry and differential scanning calorimetry (DSC). Specific heat capacities of two polymorphic forms were measured in the adiabatic calorimeter, where the β-form was measured from 10 K to 370 K and the α-form was measured from 175 K to 370 K. The start of the measurement of the stable β-form from 10 K allowed the calculation of its entropy, so we report the derived values of absolute entropy for the two forms of tristearin at 298.15 K. The enthalpies of fusion and melting temperatures for each polymorph were calculated from both the adiabatic and the DSC experimental data and are compared to the literature values. The values for the enthalpies of fusion of the stable β-form are in excellent agreement, being (221.6 ± 1) J·g^{-1} and (219.6 ± 2) J·g^{-1} according to the adiabatic and DSC measurements, respectively. The data for the α-form are not in so good agreement, which we attribute to the difficulty to crystallize this phase in its pure form. Moreover, we examined the fleeting existence of the β'-form and its transformation to the β-phase under isothermal conditions.

Introduction

Glycerides form an important class of natural products, as they are constituents of oils and fats. A very detailed review of the thermal properties of the acylglycerides is found in the chapter written by Hagemann in the Surfactant Science Series.[1] Glycerol trioctadecanoate ($C_{57}H_{110}O_6$), or tristearin for short, often indicated as SSS, is one of the saturated monoacid triglycerides and is probably the best researched triglyceride concerning thermal behavior. Despite this fact, we undertook this research as we feel that the combination of adiabatic calorimetry and DSC can give more precise data and a better insight in the crystallization processes. Moreover, the use of adiabatic calorimetry made it possible to start the measurements at such a low temperature that the absolute entropy of the stable phase could be calculated. Tristearin exhibits four polymorphic forms (α, β_2', β_1', and β), which have been identified by different techniques, like X-ray studies,[2−12] DSC,[7−18] Raman spectroscopy,[11] calorimetry,[20−22] and microscopy.[23] In this work, we observed the existence of two β'-forms by DSC, but the small temperature range in which the β_2'-phase occurred prevented detailed measurements on this form. In previous publications, we reported on the thermal properties of trielaidin[25] (or EEE) and tripalmitin[26] (or PPP). This work is part of a research project aimed at the study of metastable crystallization of binary mixtures, tristearin being one of the possible constituents.

* Corresponding author e-mail: m.matovic@chem.uu.nl.

Experimental Section

Tristearin was purchased from Larodan with a stated mass fraction purity of >99 %. The compound was used as received. The DSC experiments were performed with a Mettler Toledo DSC 821^e, equipped with an intracooler. Samples of (2 to 3) mg were used in sealed aluminum crucibles.

The adiabatic calorimeter (laboratory indication CAL8) has been described in detail before;[27] a sample of about 0.5 g was used. We estimate from calibration experiments that the uncertainty in the heat capacity measurements is within 0.5 % and that in latent heat effects, such as melting, it is about 0.2 %. Oxford Instruments calibrated the thermometer based on ITS-90. The measuring procedure consisted of alternating stabilization periods and heat input periods under automatic control. The re-crystallization effects occurring in tristearin are often so slow that equilibrium is not reached within a reasonable experiment time. In these cases, the enthalpy path of the vessel and the product were calculated by using the supplied electrical energy, corrected for the heat exchanged with the surroundings, as described in detail earlier.[28]

Results and Discussion

DSC Experiments. (a) First Melting. Tristearin, received in a solid state, was heated at a rate of 5 K·min^{-1} from the room temperature to 363 K. One endothermic peak was observed, indicating the melting of the stable

10.1021/je050092d CCC: $30.25
Published on Web 06/29/2005

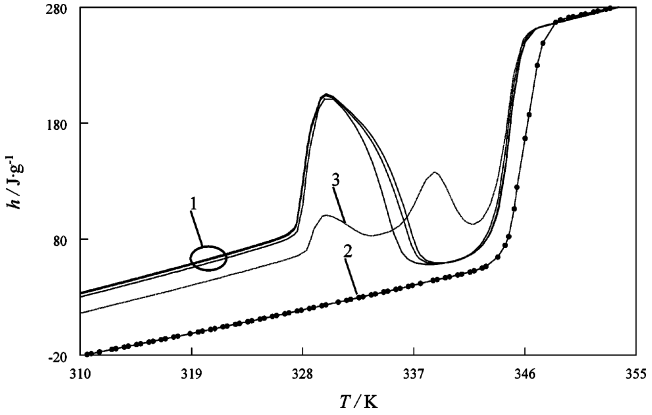

Figure 1. Pseudo-enthalpy heating curves of the solid states formed under various cooling rates. Curves 1 present the α-polymorph formed under the cooling rates of (−1, −5, and −10) K·min^{-1}, where lower energy level corresponds to a lower cooling rate. Curves 2 and 3 represent solid states both formed under the cooling rate of −0.1 K·min^{-1}.

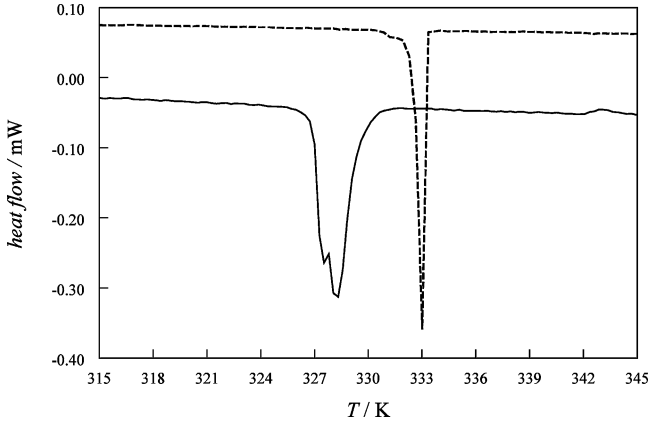

Figure 2. Crystallization of tristearin, starting at 334 K (dashed line) and 329 K (solid line) and at during the cooling of the melt with a rate of −0.1 K·min^{-1}.

β-phase. The onset of melting was at 346 K, and the enthalpy of fusion was found to be 219.6 J·g^{-1}.

(b) Influence of the Cooling Rate. To examine the occurrence of the known polymorphic forms of tristearin, several sets of experiments were performed as follows: the sample was heated with the rate of 5 K·min^{-1} to (10 to 15) K above the melting temperature of the β-phase; subsequently in each experimental set the melt was cooled at a different rate, being (−10, −5, −1, and −0.1) K·min^{-1}. The scanning patterns of the solid phases formed under these various cooling rates were recorded from 273 K at a heating rate of 5 K·min^{-1} and were transformed into pseudo-enthalpy curves (presented in Figure 1). These curves are obtained by integration of the registered heat-flow signals over time and matching the enthalpy levels in the liquid phase. By applying higher cooling rates, tristearin crystallizes in the α-polymorph which melting behavior is presented by the group of curves 1 in Figure 1. The first endothermic effect at 327 K indicates the melting of the α-form, followed by a broad exothermic peak due to the crystallization of the β′-phase from the α-melt. However, the β′-phase converts readily into the β-phase that melts at the temperature lower than that reported from the melting experiment with the sample as delivered. As already noted,[22] the melting temperature of the β-phase is dependent on the manner of preparation. As for the phase obtained from a melt, if rapidly prepared it exhibited a lower melting point, due to defects built in crystals of the β-phase.

Although crystallized at different cooling rates, the α-phase always crystallized in the vicinity of 326.6 K. The onset of melting of the α-phase (327 K) coincides with this value, meaning that no significant undercooling is needed for the nucleation of the α-form. The absence of undercooling for the α-phase has already been discussed,[24,29] while it is also observed during measurements in the adiabatic calorimeter (Figure 8, curve 1).

The curves 2 and 3 in Figure 1 present the scanning patterns of the solid forms that crystallized during cooling of the melt with the rate of −0.1 K·min^{-1}. Despite the same cooling rate, the crystallization occurred at different temperatures, resulting in different solid states. The solid phase that solidifies at 334 K exhibits only one endothermic peak on the scanning pattern, indicating that tristearin crystallized in the β-form upon slow cooling of the melt, as also concluded by Perron et al.[29] However, the crystallization occurred also at 329 K under the same cooling rate and the formed solid consisted of more than one polymorph. The scanning pattern of this solid phase (curve 3, Figure 1) demonstrates three endothermic effects, where the newly identified peak at 337.5 K corresponds to the melting of one of the β′-polymorphs. We suppose that part of the melt crystallizes in one of the β′-forms, but under constant cooling of −0.1 K·min^{-1}, the crystallization of the β′-polymorph does not go to completion and the remaining liquid crystallizes in the α-form.

According to Figure 2, the crystallization process that took place at 334 K was appreciably faster than the one occurring at 329 K under the same cooling rate. The nucleation rate of the β-form is very low, but once the β-nuclei are formed, instant crystallization follows. On the other hand, due to the slow nucleation kinetics of the β-form, the melt can easily be undercooled below the onset of the β-form crystallization, leading to the nucleation of the less stable polymorphs. In this case, the onset of crystallization occurred at lower temperature (329 K), while the shape of recorded exothermic peak points to two-step crystallization (see Figure 2). Eventually, the final solid state consists of both the α- and the β′-polymorphs.

Clearly, the influence of the applied cooling rate is evident in the final energy level of the compound. Faster cooling provides high-energy solid forms (curves 1, Figure 1), while slower cooling results in a lower energy state of the final solid (curves 2 and 3).

These observations, supported by the adiabatic measurements presented below, point to the necessity of very slow cooling of the melt in order to obtain nuclei of the β-form. They also illustrate the essential impact of kinetics on the crystallization of tristearin, which is typical for the solidification of triglycerides. The discussed influence of the cooling rate showed that principally the α-form crystallizes when the melt is cooled fast enough, while only for very low cooling rates the crystallization of the β-form is to be expected. In between, we are left with a range of cooling rates where there is a possibility that tristearin solidifies in more than one polymorphic form.

(c) Isothermal Crystallization of Tristearin into the β′-Phase. Before the β_1'- and β_2'-forms of tristearin were identified and measured as separate phase entities, there was a discussion in the literature about the different stabilities of β′-polymorphs for odd and even triglycerides.[5] These studies indicated that the β′-form of even triglycerides were decidedly more fleeting and thus are more difficult to characterize.

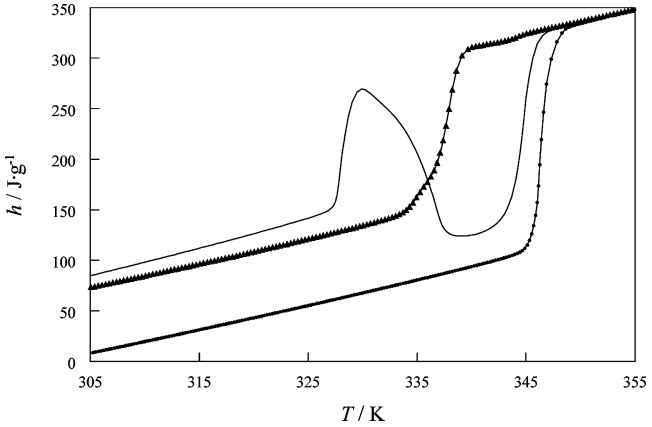

Figure 3. Pseudo-enthalpy paths of the three polymorphs of tristearin measured upon constant heating at 5 K·min^{-1}: —, α-form; ▲, β_2'-form; ●, β-form.

The enthalpy path of the α-phase (Figure 1, curve 1) shows that the melting of the α-phase is followed by the re-crystallization of the β'-form, but the melting peak of the β'-form could not be detected due to the interference of the $\beta' \rightarrow \beta$ re-crystallization. Previous studies on fat crystallization[24] suggested that the pure β'-polymorph could be formed by rapid cooling of the melt to (1 or 2) K above the α-melting point and stabilizing at that temperature for 30 min to 1 h. Therefore, we cooled the melt using a cooling rate of −10 K·min^{-1} to 329 K and left the sample at this temperature for 40 min. After cooling the obtained solid to 273 K, the heating was performed under a scanning rate of 5 K·min^{-1}. The recorded scanning pattern corresponds to that of the β_2'-form reported by Simpson and Hagemann,[11] showing two endothermic peaks that indicate the melting of the β_2'-phase at 334 K and of the β_1'-phase at 338 K. The energy level of the stable β_2'-form, prepared in the described way, falls between the levels of the α- and the β-phase, as illustrated in Figure 3. The value for the enthalpy of fusion of the β_2'-polymorph (see Table 6) is calculated as the difference between the extrapolated enthalpy levels of the liquid and the solid phase at the melting point of the β_2'-form.

However, when the α-form was heated to the same temperature of 329 K and its melt left there for 40 min, then the preparation of the β'-form failed. On scanning the obtained solid, only one endothermic peak occurred at 345 K, demonstrating the melting of the β-form. For comparison between the α-melt induced crystallization and the crystallization from the undercooled melt, the heat flows registered in both cases during the isothermal crystallization at 329 K are given in Figure 4. Accordingly, the crystallization of the β'-form requires no induction time when generated in the α-melt, but it converts readily to the β-form as can be seen from the second heat effect in the relevant curve. On the other hand, the crystallization of the β'-phase from the undercooled melt has a delay, there is a time interval during which β'-nuclei are formed. The β'-polymorph, obtained in such a way, does not transform so easily to the β-form. The higher stability of the β'-form crystallized directly from the melt as compared to the one induced from the α-melt was already reported.[19]

(d) Phase Stability of the β′-Polymorph. To get more insight into the fleeting existence of the β'-phase the following set of isothermal crystallization experiments were done at respectively (328.15, 329.15, and 330.15) K. First the sample was heated to 373.15 K in order to melt it completely and to remove possible crystallization grains. Then it was cooled at a rate of −10 K·min^{-1} to the stabilization temperature and kept at that temperature for respectively 30 min, 1 h, 2 h, and 4 h. After the stabilization period the sample was cooled to 273.15 K and was subsequently scanned to 373.15 K at a heating rate of 5 K·min^{-1}. In Figures (5a,b to 7a,b), the results are given, where the observed exothermic heat effects during the stabilization are given in the a panels and the heating scans are given in the b panels. The stabilization temperatures were chosen to be above the melting/crystallization temperature of the α-phase and below the temperature where β crystallization was observed in the adiabatic experiments. At the chosen stabilization temperatures, there is a considerable undercooling of the β as well as of the β'-phase; however, in all cases the β'-phase did crystallize first.

Typically, the crystallization of the β'-phase from the undercooled melt was appreciably faster at lower temperatures. Indication that solidification was not complete during the isothermal period is the melting peak of the

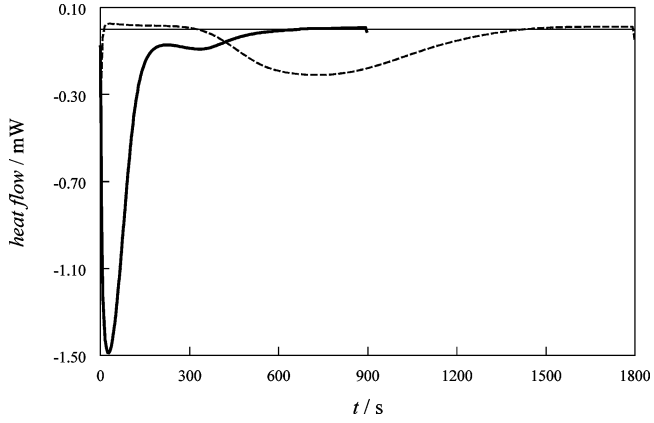

Figure 4. Isothermal crystallization of tristearin at 329 K from the α-melt (solid line) and from the undercooled melt (dashed line).

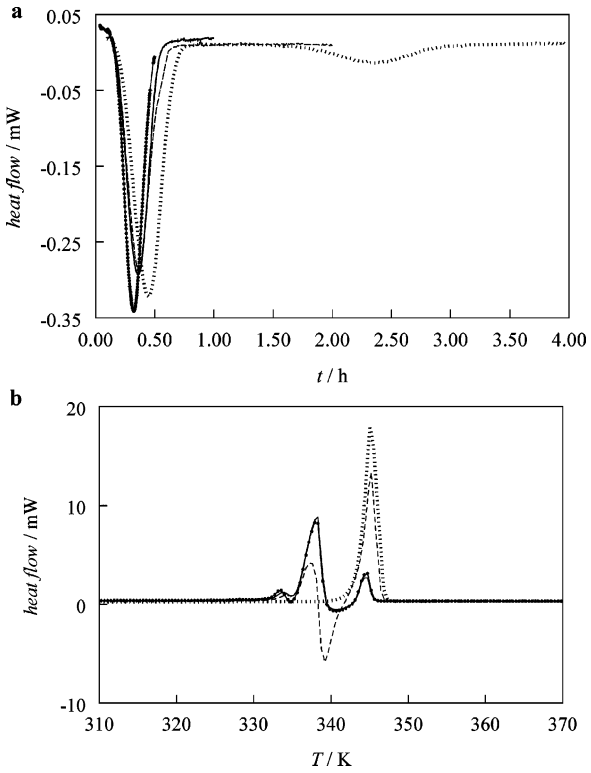

Figure 5. Isothermal crystallization of tristearin at 328.15 K: ●, 30 min; —, 1 h; – – , 2 h; · · ·, 4 h. (Panel a) Exothermic effects registered for different stabilization period. (Panel b) Heating scans of the solids formed during the corresponding period.

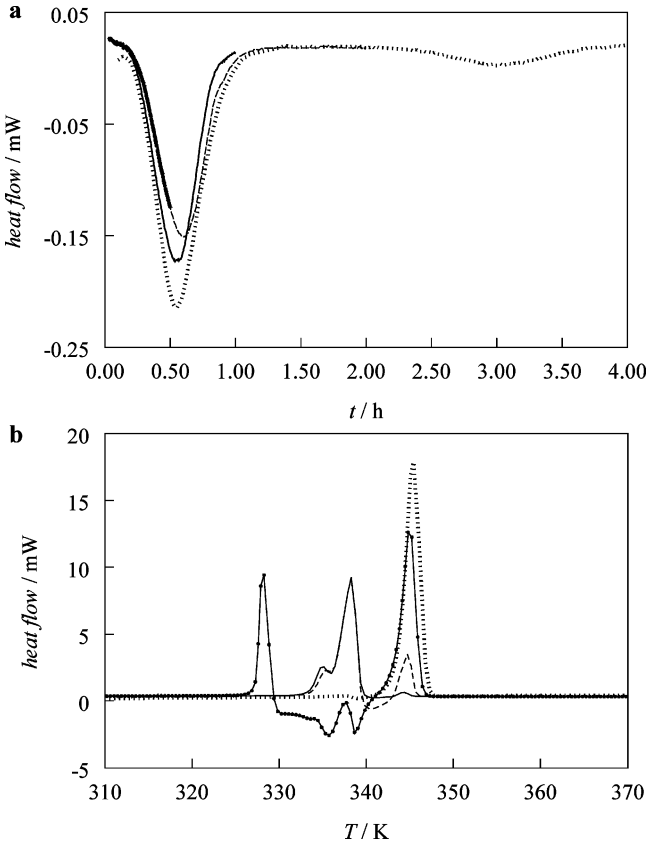

Figure 6. Isothermal crystallization of tristearin at 329.15 K: ●, 30 min; —, 1 h; – –, 2 h; · · ·, 4 h. (Panel a) Exothermic effects registered for different stabilization periods. (Panel b) Heating scans of the solids formed during the corresponding periods.

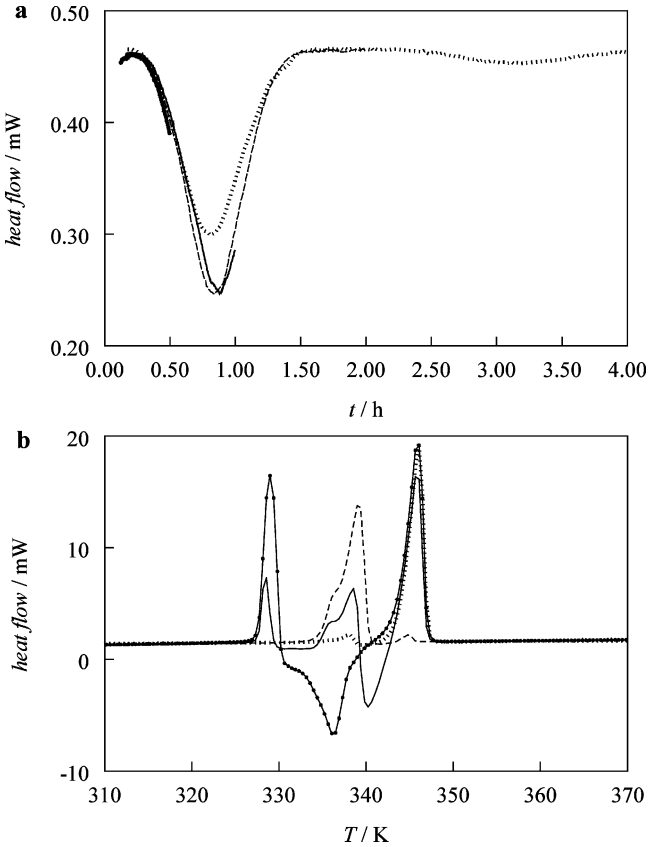

Figure 7. Isothermal crystallization of tristearin at 330.15 K: ●, 30 min; —, 1 h; – –, 2 h; · · ·, 4 h. (Panel a) Exothermic effects registered for different stabilization periods. (Panel b) Heating scans of the solids formed during the corresponding periods.

α-phase that occurs on the scanning pattern. For instance, no α-phase was observed in the solids formed at 328.15 K (Figure 5b), while after 30 min at 329.15 K an amount of liquid remained that solidified in the α-phase upon cooling to 273 K (Figure 6b). Independently of the investigated temperatures, once the β'-phase was formed it converted to the β-phase. However, the rate of $\beta' \rightarrow \beta$ transition depends on the temperature, being slower at higher temperatures. The sample kept for 4 h at 328.15 K totally transformed to the β-phase, while when it was kept at 330.15 K for the same time some amount of the β'-phase remained.

The stable β-phase can be prepared by very slow cooling of the liquid, as will be demonstrated in the adiabatic calorimeter experiment below, or by first forming the β'-phase and allowing the formed solid sufficient time to transform to the β-phase. In light of very slow nucleation rate for the β-form, these observations suggest that it would be easier to prepare the most stable phase via the intermediate β'-phase than by direct crystallization from the undercooled melt.

Adiabatic Calorimetry. (a) Crystallization from the Melt. In the adiabatic calorimeter each of the three crystalline forms studied could be crystallized from the melt. The cooling curves are shown in Figure 8, the experimental time values of the different curves were scaled in order to plot them on one axis. The scaling factor is given in the figure caption. When the sample in the adiabatic calorimeter was cooled at a rate or 16 $K \cdot h^{-1}$ or faster, the α-phase crystallized. The onset of the crystallization was at 326.3 K, remarkably no undercooling was observed (curve 1, Figure 8). This behavior is very much alike the crystallization process in long chain paraffins,

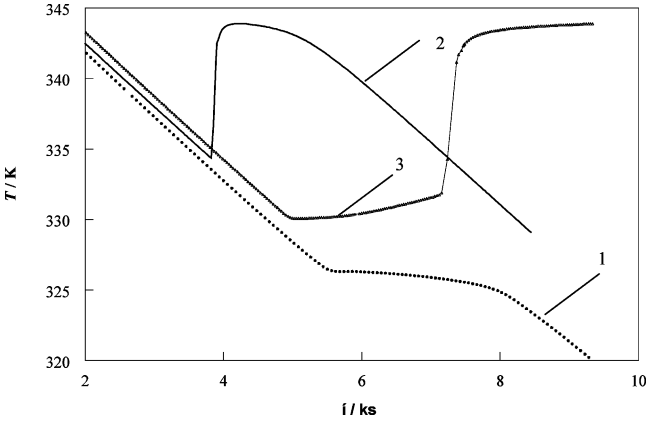

Figure 8. Cooling curves: ●, curve 1 registered upon continuous cooling at 16 $K \cdot h^{-1}$, leading to the formation of the α-phase; —, curve 2 for cooling at 3.4 $K \cdot h^{-1}$, leading to crystallization of the β-phase, the time values of this curve were divided by (16/3.4) to plot it on the same scale; △, curve 3 for cooling at 16 $K \cdot h^{-1}$, but stopped at 330 K, followed by slow crystallization to the β'-phase, at 331.9 K a sudden crystallization of the β-phase took place.

where the lack of undercooling is probably due to the formation of a crystalline monolayer on the surface of the liquid, a few degrees above the melting point.[30] We think that a similar process is involved here. The second curve in Figure 8 was made with a cooling rate of 3.4 $K \cdot h^{-1}$, in this case spontaneous crystallization of the β-phase occurred at 334.4 K. The third curve was again made at 16 $K \cdot h^{-1}$, but in this case adiabatic conditions were restored, and the cooling process was interrupted at 330 K. Under the adiabatic conditions, the influx of energy from the surroundings should not result in a visible temperature

Table 1. Experimental Heat Capacities of the Stable *β*-Phase from 10 K to 370 K

T	c_p	T	c_p	T	c_p	T	c_p
K	J·K^{-1}·g^{-1}	K	J·K^{-1}·g^{-1}	K	J·K^{-1}·g^{-1}	K	J·K^{-1}·g^{-1}
Series 1		30.62	0.176	143.02	0.830	283.16	1.520
297.32	1.609	Series 4		145.92	0.852	286.11	1.538
298.40	1.611	30.93	0.168	148.83	0.863	289.07	1.556
299.84	1.632	33.29	0.207	151.73	0.873	292.03	1.584
301.82	1.653	35.42	0.230	154.64	0.887	294.99	1.602
303.79	1.674	37.51	0.242	157.55	0.890	297.96	1.625
305.75	1.692	39.73	0.252	160.46	0.918	300.94	1.645
307.70	1.709	41.97	0.269	163.37	0.927	Series 6	
309.65	1.723	44.25	0.295	166.29	0.940	304.05	1.670
311.60	1.741	46.55	0.307	169.20	0.952	306.72	1.699
313.55	1.761	48.96	0.330	172.12	0.961	308.94	1.716
315.49	1.772	51.41	0.350	175.04	0.976	311.17	1.732
317.43	1.793	53.88	0.373	177.95	0.985	313.39	1.751
319.37	1.826	56.39	0.398	180.87	0.999	315.61	1.768
321.32	1.842	58.93	0.418	183.79	1.011	317.83	1.793
323.27	1.862	61.51	0.442	186.70	1.034	320.05	1.822
325.23	1.887	64.13	0.466	189.62	1.053	322.28	1.846
327.20	1.907	66.78	0.487	192.54	1.074	324.50	1.869
329.17	1.931	69.45	0.507	195.45	1.091	326.72	1.899
331.15	1.960	72.14	0.525	198.37	1.095	328.95	1.922
333.14	1.988	74.85	0.543	201.29	1.119	331.17	1.953
335.14	2.030	77.59	0.562	204.21	1.131	333.40	1.992
337.14	2.068	80.34	0.577	207.13	1.138	335.63	2.031
Series 2		83.10	0.595	210.05	1.148	337.85	2.073
9.65	0.009	85.88	0.612	212.96	1.155	340.08	2.142
9.71	0.014	88.67	0.626	215.88	1.164	342.28	2.395
10.85	0.025	91.47	0.642	218.80	1.172	344.14	8.560
12.51	0.030	Series 5		221.72	1.176	345.13	54.85
13.96	0.037	85.71	0.606	224.64	1.186	345.47	144.88
15.56	0.049	88.61	0.622	227.55	1.197	345.62	278.92
17.30	0.070	91.44	0.635	230.47	1.212	345.71	439.05
19.33	0.078	94.27	0.649	233.39	1.228	345.76	998.91
21.58	0.092	97.11	0.657	236.30	1.242	345.79	1233.21
23.86	0.113	99.95	0.670	239.22	1.258	345.86	285.47
26.19	0.131	102.80	0.685	242.14	1.272	346.95	3.418
28.56	0.154	105.65	0.687	245.06	1.289	349.12	2.211
30.99	0.178	108.50	0.691	247.98	1.307	351.37	2.211
Series 3		111.36	0.704	250.90	1.321	353.63	2.216
9.60	0.012	114.22	0.718	253.82	1.338	355.89	2.223
11.58	0.025	117.09	0.731	256.74	1.355	358.16	2.228
13.59	0.034	119.95	0.742	259.67	1.371	360.45	2.235
15.41	0.044	122.82	0.753	262.60	1.389	362.74	2.241
17.41	0.057	125.70	0.763	265.53	1.407	365.05	2.249
19.45	0.074	128.58	0.775	268.46	1.426	367.37	2.252
21.54	0.089	131.46	0.818	271.39	1.442	369.71	2.261
23.71	0.110	134.35	0.818	274.33	1.460		
25.95	0.129	137.23	0.804	277.27	1.489		
28.25	0.152	140.13	0.817	280.21	1.502		

increase on the scale used in this Figure. The temperature however did slowly increase, indicating that a crystallization process took place, most probably to one of the *β*′-phases. At 331.9 K, the slow increase suddenly changed and the sample crystallized to the *β*-phase. Direct formation of the *β*′-phase in the calorimeter was thus excluded as the crystallization process raises the temperature to a value where crystallization to the *β*-phase takes place.

(b) The β-Phase. From the DSC experiment, we knew that the sample as received was in the *β*-form. To allow optimum relaxation of this crystal form, the sample was first heated till about 2 K below the melting point of the stable *β*-polymorph. At this temperature the sample was stabilized for 24 h before cooling to liquid helium temperature. In Table 1, the subsequent measurements from (10 K to 370 K) are given. The heat capacity curves of this phase and of the other polymorphs discussed below are shown in Figure 10. Around 130 K a small, unexplained hump in the data is observed, we repeated the measurements in this temperature region twice with the same result. The absolute entropy s_{abs} and melting enthalpy $h(T)-h(0)$ of the *β*-polymorph were calculated by numerical integration. The starting values of this integration were calculated at 10 K by assuming that below this temperature the Debye low-temperature limit for the heat capacity could be applied. The thermodynamic functions are given in Table 2 at selected temperatures. The enthalpy of fusion of the *β*-phase was measured twice; the mean value was (221.6 ± 1) J·g^{-1}, and the triple point value was found to be (345.94 ± 0.01) K. In Table 3, the results of the two melting experiments are given, together with the linear fits

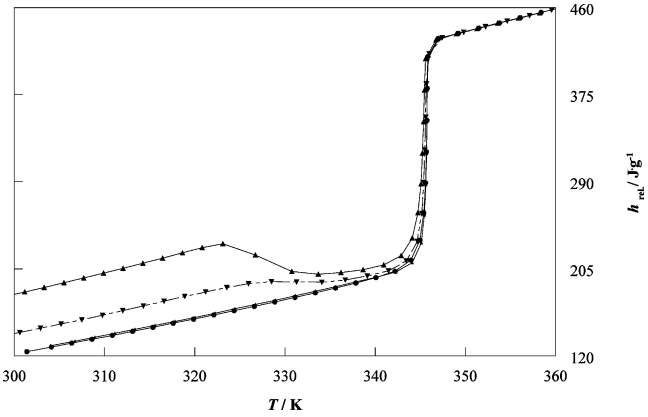

Figure 9. Experimental relative enthalpy curves: ▲, α-phase; ●, *β*-phase; ▼, the solid formed by annealing the melt at 328 K for 4 h. The curves are shifted so that they coincide in the liquid phase.

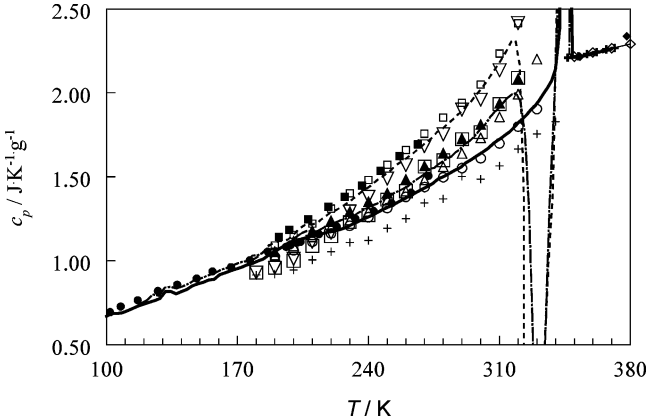

Figure 10. Comparing the experimental heat capacity curves of tristearin with literature data: α-phase: - -, this work; □, Simpson;[17] ▽, Hampson and Rothbart;[18] ■, Charbonnet and Singleton.[20] *β*-phase: —, this work; ○, Simpson;[17] +, Hampson and Rothbart;[18] ●, Charbonnet and Singleton.[20] *β*′-phase: - · -, this work; △, (β_1′) Simpson;[17] ▲, (β_2′) Simpson;[17] □, Hampson and Rothbart.[18] Liquid phase: —, this work; ◇, Morad et al.;[15] ◆, Phillips and Mattamal;[16] +, Charbonnet and Singleton[20].

Table 2. Derived Thermodynamic Properties of the *β*-Form of Tristearin at Selected Temperatures

T	c_p	s_{abs}	$h-h(0)$	T	c_p	s_{abs}	$h-h(0)$
K	J·K^{-1}·g^{-1}	J·K^{-1}·g^{-1}	J·g^{-1}	K	J·K^{-1}·g^{-1}	J·K^{-1}·g^{-1}	J·g^{-1}
10	0.019	0.006	0.05	200	1.109	1.154	120.7
20	0.068	0.036	0.50	210	1.148	1.209	132.0
30	0.170	0.084	1.72	220	1.174	1.263	143.6
40	0.254	0.146	3.91	230	1.210	1.316	155.5
50	0.338	0.212	6.88	240	1.262	1.368	167.8
60	0.428	0.282	10.71	250	1.317	1.421	180.7
70	0.510	0.354	15.43	260	1.373	1.474	194.2
80	0.575	0.427	20.87	270	1.434	1.527	208.2
90	0.628	0.498	26.90	280	1.501	1.580	222.9
100	0.671	0.566	33.39	290	1.564	1.634	238.2
110	0.697	0.631	40.25	298.15	1.626	1.678	251.2
120	0.743	0.694	47.46	300	1.639	1.688	254.2
130	0.796	0.755	55.08	310	1.724	1.743	271.0
140	0.817	0.815	63.21	320	1.821	1.799	288.7
150	0.867	0.873	71.64	330	1.935	1.857	307.5
160	0.915	0.931	80.50	340	2.140	1.917	327.7
170	0.955	0.987	89.84	350	2.211	2.612	567.7
180	0.994	1.043	99.58	360	2.233	2.675	589.9
190	1.056	1.098	109.8				

Table 3. Melting of the *β*-Phase of Tristearin

used linear functions of heat capacity	temperature interval	Δh_{fus}
$J \cdot K^{-1} \cdot g^{-1}$	K	$J \cdot g^{-1}$
c_p (solid, 300 K−317 K) = −0.664 + 0.00768 *T*/K	317 to 349	220.9 (first melt)
c_p (liquid, 350 K−365 K) = 1.264 + 0.00267 *T*/K		222.4 (second melt)
mean value		221.6 ± 1

Table 4. Experimental Heat Capacities and Enthalpy Increment of the α-Phase of Tristearin

T	c_p	*h*(T)−*h*(0)	*T*	c_p	*h*(T)−*h*(0)
K	$J \cdot K^{-1} \cdot g^{-1}$	$J \cdot g^{-1}$	K	$J \cdot K^{-1} \cdot g^{-1}$	$J \cdot g^{-1}$
178.91	1.010	134.09	283.59	1.828	279.67
181.60	1.030	136.87	285.80	1.848	283.72
184.26	1.057	139.63	288.00	1.874	287.82
186.88	1.093	142.40	290.20	1.895	291.96
189.48	1.106	145.24	292.39	1.925	296.15
192.06	1.117	148.11	294.59	1.944	300.40
194.63	1.120	150.99	296.78	1.978	304.70
197.18	1.128	153.86	298.97	2.005	309.06
199.71	1.155	156.75	301.16	2.037	313.47
202.23	1.182	159.69	303.34	2.069	317.97
204.74	1.205	162.68	305.53	2.106	322.53
207.23	1.222	165.70	307.71	2.142	327.16
209.71	1.215	168.72	309.89	2.179	331.88
212.17	1.224	171.72	312.07	2.217	336.66
214.62	1.246	174.75	314.26	2.259	341.54
217.06	1.265	177.81	316.44	2.307	346.52
219.48	1.287	180.90	318.63	2.316	351.60
221.90	1.298	184.02	320.84	2.169	356.55
224.30	1.313	187.15	323.13	1.384	360.60
226.69	1.330	190.31	326.73	−5.225	349.59
229.06	1.347	193.49	330.77	−2.092	333.57
231.43	1.366	196.70	333.70	0.373	330.65
233.79	1.389	199.94	336.23	0.983	332.35
236.13	1.409	203.22	338.66	1.437	335.29
238.46	1.426	206.53	340.96	2.653	339.93
240.79	1.445	209.86	342.89	7.391	348.96
243.10	1.467	213.23	344.13	26.47	366.17
245.41	1.489	216.64	344.75	66.64	390.88
247.71	1.503	220.08	345.07	126.87	419.16
250.00	1.524	223.54	345.26	210.24	449.01
252.28	1.544	227.04	345.38	312.73	479.63
254.56	1.568	230.58	345.47	400.99	510.65
256.83	1.585	234.16	345.60	167.56	541.20
259.09	1.600	237.76	346.77	3.134	559.55
261.34	1.620	241.39	349.01	2.220	565.50
263.59	1.639	245.05	351.31	2.208	570.59
265.83	1.659	248.75	353.61	2.212	575.66
268.07	1.677	252.47	355.92	2.218	580.78
270.30	1.700	256.24	358.24	2.223	585.93
272.53	1.719	260.05	360.57	2.230	591.12
274.75	1.742	263.89	362.91	2.241	596.35
276.96	1.770	267.78	365.27	2.244	601.64
279.18	1.784	271.70	367.64	2.250	606.95
281.39	1.806	275.67	370.02	2.257	612.32

of the heat capacity of the solid and the liquid phase around the melt used in the calculation. From the plot of the equilibrium temperatures in the melt against the reciprocal of the melted fraction, the purity of the sample was calculated to be (97.9 ± 0.1) mol %.

(c) The α-Phase. Cooling the sample from the liquid phase at a rate of 16 $K \cdot h^{-1}$ or larger resulted in the formation of the α-phase. On heating the obtained solid from 175 K, the heat capacity of the α-phase is measured and the transition of α → *β* → liquid is observed. The experimental heat capacity data are given in Table 4. As in the measured temperature range exothermic effects occurred due to re-crystallization, we did include the relative enthalpy values in this table. The enthalpy values of the measuring set starting in the α-phase were shifted, so that they coincide in the liquid phase with the enthalpy values of the liquid phase obtained from the measurement of the stable *β*-phase. As can be seen in Figure 10, the heat capacity of the α-phase increases rather sharply before the melting point. In the adiabatic calorimetry experiments the transition of the α-phase to the *β*-phase or the *β*′-phase started already before the melting point of the α-phase was reached. At the melting temperature of the α-phase, being 326.6 K according to the DSC experiments, the formed liquid is directly transformed to the *β*- or the *β*′-phase. In Figure 9 the relative enthalpy curves of the different phases are given. From this picture it is clear that within the experimental time used, the transition to the *β*-phase was not completed, and it is only at the very end of the melting process of the *β*-phase that the curves coincide.

(d) The β′-Phase. The results from the isothermal experiments in the DSC explain why in the adiabatic calorimeter experiments the *β*′-phase could not be observed. These adiabatic measurements are so slow that the sample has transformed to the *β*-phase before the melting point of the *β*′-phase was reached. To measure the *β*′-phase in the adiabatic calorimeter, we removed the vessel from the calorimeter, immersed it in hot water to melt the contents and transferred it to a temperature regulated block. The vessel was kept at 328 K for 4 h, then cooled to room temperature and replaced in the calorimeter.

Although the DSC experiments showed that after 4 h the whole sample would convert to the *β*-phase, hereby we point to the essential influence of the mass of tristearin that is annealed in order to obtain the *β*′-form. The whole amount of the sample of 1.55 mg in the DSC experiment would crystallize in the β_2'-form within 40 min at 328 K, but it transformed to the *β*-phase while staying at the given temperature for 4 h. The β_2'-phase, for which the heat capacity is shown in Figure 10,[11] was formed in a capillary tube by annealing the melt at 328 K for 15−25 min. Hence, the optimal annealing time for obtaining the pure *β*′-form depends on a sample size.

The heat capacity of the solid formed outside the calorimeter is presented in Figure 10. The values are intermediate to the curves for the α- and the *β*-phase, but we cannot be sure whether it is due to the formation of the pure *β*′-phase or if the measured solid was actually a mixture of the α-phase and one or two of the other polymorphs. We believe that the α-phase is present as the re-crystallization starts at the melting temperature of the α-phase (see Figure 10). More detailed characterization of the solid structure is not possible by using only thermal analysis, thus we cannot give reliable heat capacity values for the *β*′-phase.

(e) Enthalpy and Entropy Values of the α- and the β-Phase at 298.15 K. The enthalpy and entropy values of the different polymorphic phases can be calculated by constructing a reversible path connected to the liquid phase. First the enthalpy of the liquid phase was extrapolated to the melting point of the α-phase by assuming that the heat capacity could be extrapolated linearly. The enthalpy of fusion of the α-phase was taken as the difference between the extrapolated enthalpy values of the liquid and the relevant solid at the melting point. Then the same procedure was repeated for the entropy, using

Table 5. Enthalpy, Entropy, and Relative Gibbs Energy Values at 298.15 K for the Two Polymorphic Forms and the Temperatures of Fusion and the Enthalpy of Fusion

	T_{fus}	Δh_{fus}	$h(298.15)-h(0)$	s_{abs}	g
phase	K	$J \cdot g^{-1}$	$J \cdot g^{-1}$	$J \cdot K^{-1} \cdot g^{-1}$	$J \cdot g^{-1}$
β	345.9	221.6	251.2	1.678	−249.1
α	327.3	144.8	307.4	1.816	−234.0

Table 6. Melting Temperatures and Enthalpies of Fusion of the Three Polymorphic Phases and Comparison with the Literature

β		β_2'		α		
T_{fus}	Δh_{fus}	T_{fus}	Δh_{fus}	T_{fus}	Δh_{fus}	
K	$J \cdot g^{-1}$	K	$J \cdot g^{-1}$	K	$J \cdot g^{-1}$	reference
						this work
345.9	221.6			327.3	144.8	adiabatic
346.0	219.6	336.7	154.2	327.3	128.0	DSC
346.6	214.7	336.4		328.1		2
344.6				327.6		3
346.1		337.1		327.3		4
345.6		337.6		327.6		7
346.7		336.1		327.8		8
		336.4	162.7			12
346.3	220.7	337.1	178.4	327.1	162.9	14
343.1						15
	70.4					19
345.7	228.0			327.1	162.8	20
345.5	213.0			326.0	153.6	21
346.3	211.4	336.7	168.9	328.3	122.6	22
345.7	216.7	337.5	175.2[a]	327.9	126.9	24

[a] Not indicated in the reference for which the β' polymorph value is given.

as the entropy of fusion the calculated enthalpy of fusion divided by the temperature of fusion. In Table 5, the calculated enthalpy and entropy values of the α- and the β-phase at 298.15 K are given, together with the calculated enthalpies of fusion.

(f) Comparing the Results. In Figure 10, the literature data for the heat capacities of the different phases are plotted. Generally the correspondence is good, especially for the liquid phase. However, the results of Hampson and Rothbart[18] significantly deviate from our data, which could be due to the relatively high heating rate of 10 $K \cdot min^{-1}$ that they used for scanning solids in the DSC. In Table 6, we compare the temperatures and enthalpies of fusion of the different phases with the literature values. Here, the correspondence is also within the error margins, except for ref 19. We think that in that case the authors integrated the DSC melting curve in the melt of the β-phase without taking into account the re-crystallization, which took place in the same run. The heat capacities of the solid formed by annealing of the melt for 4 h at 328 K, obtained from the adiabatic measurement, are plotted in Figure 10. They correspond quite well to the literature data of the β'-form. Nevertheless, we do not exclude the possibility that the relevant solid phase could be the mixture of more polymorphs in such a ratio that the heat capacity values coincide with that of the β'-phase.

Literature Cited

(1) Hagemann, J. W. Thermal behaviour and polymorphism of acylglycerides. *Crystallization and Polymorphism of Fats and Fatty Acids*; Garti, N., Sato, K., Eds.; Surfactant Science Series 31; Marcel Dekker: New York, 1988; pp 9−95.

(2) Kodali, R. D.; Atkinson, D.; Redgrave, T. G. Small, D. M. Structure and polymorphism of 18-carbon fatty acyl triacylglycerols: effect of unsaturation and substitution in the 2-position. *J. Lipid Res.* **1987**, *28*, 403−413.

(3) Clarkson, C. E.; Malkin, T. Alternation in long-chain compounds. Part II. An X-ray and thermal investigation of the triglycerides. *J. Chem. Soc.* **1934**, 666−671.

(4) Lutton, E. S. Phase behavior of triglyceride mixtures involving primarily tristearin, 2-oleyldistearin and triolein. *J. Am. Oil Chem. Soc.* **1955**, *32*, 49−53.

(5) Lutton, E. S.; Fehl, A. J. The polymorphism of odd and even saturated single acid triglycerides C_8−C_{22}. *Lipids* **1970**, *5* (1), 90−99.

(6) Cebula, D. J.; Smith, P. R. Dynamic polymorphic phase transitions in a model binary triglyceride system measured by position-sensitive X-ray diffraction methods. *J. Am. Oil Chem. Soc.* **1990**, *67*, 811−814.

(7) Lavigne, F.; Bourgaux, C.; Ollivon, M. Phase transitions of saturated triglycerides. *J. Phys. IV, Proc.* **1993**, *3*, 137−140.

(8) Whittam, J. H.; Rosano, H. L. Physical aging of even saturated monoacid triglycerides. *J. Am. Oil Chem. Soc.* **1975**, 128−133.

(9) Hagemann, J. W.; Rothfus, J. A. Polymorphism and transformation energetics of saturated monoacid triglycerides from differential scanning calorimetry and theoretical modeling. *J. Am. Oil Chem. Soc.* **1983**, *60*, 1123−1131.

(10) Oh, J. H.; McCurdy, A. R.; Clark, S.; Swanson, B. G. Characterization and thermal stability of polymorphic forms of synthesized tristearin. *J. Food Sci.* **2002**, *67*, 2911−2917.

(11) Simpson, T. D.; Hagemann, J. W. Evidence of two β' phases in tristearin. *J. Am. Oil Chem. Soc.* **1982**, *59*, 169−171.

(12) Kellens, M.; Reynaers, H. Study of the polymorphism of saturated monoacid triglycerides. II: polymorphic behaviour of a 50/50 mixture of tripalmitin and tristearin. *Fat Sci. Technol.* **1992**, *94* (8), 286−293.

(13) Walker, W. W. Aging of tristearin: comparison of DSC and positron lifetime results. *J. Am. Oil Chem. Soc.* **1987**, *5*, 754−756.

(14) Perron, R. R. Commentaires sur le comportement thermique des triglycerides—role de l'insaturation. *Rev. Fr. Corps Gras* **1984**, 171−179.

(15) Morad, N. A.; Idrees, M.; Hasan, A. A. Specific heat capacities of pure triglycerides by heat-flux differential scanning calorimetry. *J. Therm. Anal.* **1995**, *45*, 1449−1461.

(16) Phillips, J. C.; Mattamal, M. M. Correlation of liquid heat capacities for the carboxylic esters. *J. Chem. Eng. Data* **1976**, *21*, 228−232.

(17) Simpson, T. D. Specific heats of the solid-state phases of trimargarin and tristearin. *J. Am. Oil Chem. Soc.* **1984**, *61* (5), 883−886.

(18) Hampson, J. W.; Rothbart H. L. Triglyceride specific heat determined by differential scanning calorimetry. *J. Am. Oil Chem. Soc.* **1983**, *60*, 1102−1104.

(19) Desmedt, A.; Culot, C.; Deroanne, C.; Durant, F.; Gibon, V. Influence of cis and trans double bonds on the thermal and structural properties of monoacid triglycerides. *J. Am. Oil Chem. Soc.* **1990**, *67*, 658−660.

(20) Charbonnet, G. H.; Singleton, W. S. Thermal properties of fats and oils. *J. Am. Oil Chem. Soc.* **1947**, 140−142.

(21) Norton, I. T.; Lee-Tuffnell, C. D.; Ablett, S.; Bociek, S. M. A calorimetric, NMR and X-ray diffraction study of the melting behavior of tripalmitin and tristearin and their mixing behavior with triolein. *J. Am. Oil Chem. Soc.* **1985**, *62*, 1237−1244.

(22) Ollivon, M.; Perron, R. Measurements of enthalpies and entropies of unstable crystalline forms of saturated even monoacid triglycerides. *Thermochim. Acta* **1982**, *53*, 183−194.

(23) Okada, M. The transformation of SSS crystal from α form to β form by melt grown method. *J. Electron Microsc.* **1964**, 180−181.

(24) Wesdorp, L. H. Liquid-multiple solid-phase equilibria in fats. Thesis, Technische Universiteit Delft, 1990.

(25) Miltenburg, J. C. van; Ekeren, P. J. van; Gandolfo, F. G.; Flöter, E. Investigation of the thermal behaviour of trielaidin between 10 K and 360 K. *J. Chem. Eng. Data* **2003**, *48*, 1245−1250.

(26) Miltenburg, J. C. van; ten Grotenhuis, E. A Thermodynamic investigation of tripalmitin. molar heat capacities of the α- and β-form between 10 K and 350 K. *J. Chem. Eng. Data* **1999**, *44*, 721−726.

(27) van Miltenburg, J. C.; van den Berg, G. J. K.; van Genderen, A. C. G. An adiabatic calorimeter for small samples. The solid−liquid system naphthalene−durene. *Thermochim. Acta* **2002**, *383*, 13−1.

(28) van Miltenburg, J. C.; van Genderen, A. C. G.; van den Berg, G. J. K. Design improvements in adiabatic calorimetry. The heat capacity of cholesterol between 10 and 425 K. *Thermochim. Acta* **1998**, *319*, 151−162.

(29) Perron, R.; Petit, J.; Mathieu, A. A study of palmitic−stearic triglycerides and their binary mixtures by differential thermal analysis. I—pure triglycerides. *Chem. Phys. Lipids* **1969**, *3*, 11−28.

(30) Wu, X. Z.; Sirota, E. B.; Sinha, S. K.; Ocko, B. M.; Deutsch, M. Surface crystallization of liquid normal-alkanes. *Phys. Rev. Lett.* **1992**, *70*.

Received for review March 9, 2005. Accepted May 31, 2005.

JE050092D